Published in final edited form as:
J Biomech. 2010 January 19; 43(2): 274–279. doi:10.1016/j.jbiomech.2009.08.039.

Early response to tendon fatigue damage accumulation in a novel in vivo model

David T. Fung, **Vincent M. Wang**, **Nelly Andarawis-Puri**, **Jelena Basta-Pljakic**, **Yonghui Li**, **Damien M. Laudier**, **Hui B. Sun**, **Karl J. Jepsen**, **Mitchell B. Schaffler**, and **Evan L. Flatow***
Leni and Peter W. May Department of Orthopaedics, Mount Sinai School of Medicine, 5 East 98th Street, 9th Floor, NY 10029, USA

Abstract

This study describes the development and application of a novel rat patellar tendon model of mechanical fatigue for investigating the early in vivo response to tendon subfailure injury. Patellar tendons of adult female Sprague-Dawley rats were fatigue loaded between 1–35 N using a custom-designed loading apparatus. Patellar tendons were subjected to Low-, Moderate- or High-level fatigue damage, defined by grip-to-grip strain measurement. Molecular response was compared with that of a laceration-repair injury. Histological analyses showed that progression of tendon fatigue involves formation of localized kinked fiber deformations at Low damage, which increased in density with presence of fiber delaminations at Moderate damage, and fiber angulation and discontinuities at High damage levels. RT-PCR analysis performed at 1- and 3-day post-fatigue showed variable changes in type I, III and V collagen mRNA expression at Low and Moderate damage levels, consistent with clinical findings of tendon pathology and were modest compared with those observed at High damage levels, in which expression of all collagens evaluated were increased markedly. In contrast, only type I collagen expression was elevated at the same time points post-laceration. Findings suggest that cumulative fatigue in tendon invokes a different molecular response than laceration. Further, structural repair may not be initiated until reaching end-stage fatigue life, where the repair response may unable to restore the damaged tendon to its pre-fatigue architecture.

Keywords

Tendon; Tendinopathy; Tendon injury; Animal model; Fatigue; Damage accumulation; Biomechanics; Morphology; Histology; Second harmonic generation; Imaging

1. Introduction

Tendinopathy and tendon rupture are common painful and debilitating clinical problems. The Achilles, patellar and rotator cuff tendons are particularly prone to tendinopathies (Kannus and Jozsa, 1991; Maffulli et al., 2004) due to their tensile overload, material and structural inhomogeneity, and poor healing response (Leadbetter, 1992; Maganaris et al., 2004; Mehta et al., 2003; Riley, 2004). Observed degenerative changes in ruptured tendons suggest pre-rupture damage accumulation (Kannus and Jozsa, 1991; Tallon et al., 2001). Additionally, matrix disorganization with cellular proliferation and lipid accumulation was

*Corresponding author. Tel.: +1 212 241 1663; fax: +1 212 427 0208. Evan.Flatow@msnyuhealth.org (E.L. Flatow).

Conflict of interest
None of the authors have any relevant commercial relationships which may lead to a conflict of interest.

observed in macroscopically “healthy” tendons from older subjects (Kannus and Jozsa, 1991), suggesting damage accumulation. It is thus thought that cumulative injury from overuse causes degeneration leading to tendon weakening and failure.

Overuse/cyclic loading protocols have been used to investigate the mechanical basis of degradation and matrix degeneration in tendons. Studies evaluating the relationship between applied stress and number of cycles to failure of devitalized tendons and ligaments showed progressive degradation of mechanical properties (Ker et al., 2000; Pike et al., 2000; Schechtman and Bader, 1997, 2002; Wang and Ker, 1995; Wang et al., 1995; Wren et al., 2003). In vivo tendon modeled overuse injuries by utilizing treadmill running, muscle stimulation and repeated reaching tasks (Backman et al., 1990; Nakama et al., 2005; Soslowsky et al., 2000) and showed tendon damage, including fiber disorganization, microtears, and reduction of modulus and maximum stress. Furthermore, inability of degenerative changes to recover with time (Soslowsky et al., 2000) indicate a poor repair response likely from disrupted collagen fibrillogenesis, which is required for the scar tissue deposition, collagen synthesis, and tissue remodeling seen in wound healing (Hiranuma et al., 1996; Oshiro et al., 2003; Sakai et al., 2001; Williams et al., 1984)). However, the *process* of microstructural damage initiation and accumulation from loading, and the resulting tendon weakening and *cellular-matrix response* should be evaluated.

Previously, we investigated fatigue-induced damage accumulation in tendons using an ex vivo model of rat flexor digitorum longus (FDL) tendons (Fung et al., 2008). Results demonstrated changes in morphology and mechanical properties representing key mechanistic events during fatigue life. In this study, we developed an in vivo animal model to evaluate tendon response to fatigue loading at various damage levels based on previous ex vivo studies. For comparison, we concurrently evaluated the response of the patellar tendon to laceration and suture-repair. We hypothesize that fatigue-induced damage in tendons does not elicit the typical healing response seen in laceration. More specifically, while the extent to which a fatigue damage tendon may undergo any structural repair is unknown, we expect that its response to fatigue damage accumulation will differ from that of a lacerated tendon in that it will not exhibit the expression spectrum of collagens that accompanies the lacerated tendon’s attempt to undergo structural repair.

2. Materials and methods

2.1. Animal model for *in vivo* fatigue loading

Our criteria for selecting an animal model were (1) a small animal previously used to investigate tendon biomechanics, tissue adaptation, and biochemical and molecular studies of tendon physiology and pathology; (2) a tendon that can be fatigue loaded with control; and (3) a tendon that exhibits tendinopathy in humans. Candidates evaluated included the FDL, Achilles, patellar, supraspinatus and tail tendons in mice, rats, rabbits and dogs.

Patellar tendons in adult female Sprague-Dawley rats (n=74; 390±30 g) (Charles River Laboratories, Ltd., Wilmington, MA, USA) were chosen because of their size and the available cellular and molecular techniques for tissue analyses. Small incisions reveal two easily gripped bony attachments to the patellar tendon allowing tendon loading without direct contact with the tendon. Additionally, patellar tendinopathy (“jumper’s knee”) is prevalent, particularly among athletes (Matheson, 2003). Furthermore, rats are well characterized for tissue analysis of tendon injury using biomechanical, histological, and molecular assays (Lin et al., 2004; Oshiro et al., 2003; Ralphs et al., 1998).

All procedures were conducted under aseptic conditions and continuous administration of isoflurane anesthesia (2–3% by volume, flow rate 0.4 L/min) under approval from the Institutional Animal Care and Use Committee.

2.1.1. Loading setup—The anesthetized rat was secured to an adjustable testing frame in the supine position, maintaining a knee flexion angle of ~30° throughout loading (Fig. 1). A longitudinal incision was made near the superior border of the patella and extended distally to expose the patellar tendon. A custom-made clamp gripped the patella between its medial and lateral aspects and was attached to a testing machine to allow for controlled loading (Instron 8841, Canton, MA, USA). A 5 mm cutaneous incision distal to the tibial tubercle was made. The tibia was gripped with a custom clamp and mounted to a 6 degree-of-freedom base, ensuring alignment of the patellar tendon with the loading axis, and fixed, allowing 0 degrees-of-freedom. Setup procedures lasted ~10 min. Gripping the patella and tibia allowed loading of the patellar tendon without any direct instrumentation of the tendon, eliminating the likelihood of tendon injury other than by tensile loading.

A 3 N preload was applied to the tendon, and initial length, L_0 (measured with calipers as the distance between the distal end of the patella and proximal tibial tuberosity) and initial actuator position, d_0, was recorded. Preliminary studies were conducted that showed that actuator displacement directly resulted in patellar tendon deformation (Fig. 2). Briefly, the deformation of scattered texture on the tendon correlated with the grip-to-grip strain (90% of the grip-to-grip movements translated into tendon deformation). Tendons were loaded using a fatigue loading protocol adapted from fatigue studies in the FDL tendon (Fung et al., 2008) and cortical bone (Jepsen and Davy, 1997). Load levels were chosen based on preliminary studies (n=16) that showed a mean tendon tensile strength of 81±11 N. Tendon and surgical field were continuously moistened with sterile phosphate buffered saline.

2.1.2. Fatigue loading—Tendons were preconditioned by cyclic loading between 1 and 11 N at 1 Hz for 6 min. Tendons were fatigue loaded between 1 and 35 N at 1 Hz using a haversine waveform, corresponding to 40±7% of the monotonic failure strength, generating a grip-to-grip strain of 4.5±0.6%. Analogous to previous ex vivo studies (Fung et al., 2008), in vivo patellar tendon peak cyclic strain ($(d_{max} - d_0)/L_0$, where d_{max} is actuator position at maximum cyclic load) was characterized by three phases (Fig. 3). Transition from Primary to Secondary phase consistently occurred between cycle 300 and 500. A 2.5–3.0% peak cyclic strain increase beyond that measured at cycle 500 corresponded to early Tertiary phase. Thus, in this study, early-, mid- and late-stage fatigue were, respectively, defined as 0.6% (Low), 1.7% (Moderate) and 3.5% (High) increase in peak cyclic strain beyond that measured at cycle 500. Following completion of the loading protocol, incisions were sutured (Proline; Ethicon, Somerville, NJ), analgesia (Buprenex) was administered and animals resumed normal cage activity.

2.1.3. Characterization of *in vivo* mechanical behavior—Mechanical behavior of the tendon was characterized by tangent stiffness (T), hysteresis (H), and peak strain magnitude specific to the fatigue damage level. For a particular loading cycle, T was computed from a linear fit of the upper 60% of the force–displacement data (r^2>0.99). Hysteresis was defined as the area bound between the loading and unloading curves. To determine effects of fatigue loading on tendon, both T and H were evaluated at the baseline cycle (cycle 15) (T_1, H_1) and at the endpoint cycle of the fatigue tests (T_2, H_2), representing initial and fatigue damaged states of the tendon, respectively. Cycle 15 was used for baseline measurements because the loading system feedback controller was consistent and precise after 12 cycles. Mechanical degradation of the tendon was defined relative to baseline values as change in stiffness ($T_{1\rightarrow 2}=(T_1 - T_2)/T_1$) and hysteresis ($H_{1\rightarrow 2}=(H_1 - H_2)/H_1$) at fatigue endpoint.

2.2. Tendon wound healing in response to laceration

Age and weight matched rats were anesthetized, and a longitudinal skin incision was made exposing the patellar tendon. A transverse, full-thickness midsubstance laceration was made in the tendon and repaired with a modified Kessler stitch using a 6-0 Proline suture. The skin incision was sutured with a 6-0 Proline, and animals resumed normal cage activity following administration of analgesia (Buprenex).

2.3. Tissue analyses

—From the fatigue loaded group, rats were randomly selected and euthanized (via CO_2 inhalation) for acute microstructural damage assessment, immediately following completion of fatigue loading (n=2/damage group and n=2/control group) and gene expression response (n=6/damage group/time point evaluated at 1- and 3-days post-fatigue). The entire laceration group was used for gene expression response analysis at 1- and 3-days post-injury (n=6/time point). Additional animals were used for sham-operated (n=6/time point, patella and tibia were exposed and clamped for 3 h, corresponding to the longest period of clamping in fatigue loaded animals, but no load was applied) and naïve controls (n=6/time point).

Microstructural studies: Quadriceps–patella–patellar tendon–tibia complexes were harvested and fixed in tension in neutral buffered formalin for 48 h. Specimens were plastic embedded for histologic evaluation (Laudier et al., 2007). For second harmonic generation imaging (SHG), Mid-sagittal thick sections (200–250 μm) were cut with a diamond wafering saw (Isomet; Buehler, Ltd., Lake Bluff, IL, USA) with a silicone-based lubricant (Eros; Megasol Cosmetic GmbH, Germany) to prevent hydration. SHG imaging was performed using an upright laser-scanning multiphoton microscope (LSM 510; Carl Zeiss, Jena, Germany), with a 9-Watt mode-locked femtosecond Ti:Sapphire laser (170-fs pulse width, 76 MHz repetition rate; Mira 900 F; Coherent Inc., Santa Clara, CA, USA), tuned to 840 nm. An oil immersion objective (NA=1.0; 40 × magnification) was used for focusing the excitation beam and for collecting the backward SHG signals which were then directed by a dichroic mirror to an external detector through a narrow bandpass filter (450/40 nm). Images were acquired at tendon midsubstance at 1024 × 1024 pixel resolution on a field of view of 400 × 400 μm at 15 lines/second and 1 μm intervals through the thickness of the section. The high power, near-infrared (long-wavelength) laser-light used in multiphoton microscopy, penetrates ~200 μm in tendon thick sections, avoiding artifacts typically associated with thin sections, eliminating the need for staining and minimizing artifacts due to tissue processing by allowing visualization of tendon collagen microstructure at depths far from the cutting surface.

Gene expression analysis: Tendons were isolated from fatigue loaded, laceration-repaired, sham and control animals at designated time points, then frozen in liquid nitrogen, pulverized and suspended in buffer. Total RNA was isolated and reverse transcribed with MMLV reverse transcriptase and an $Oligo(dT)_{12–18}$ primer. Real-time PCR-amplified cDNA was quantified by fluorescence using the ABI Prism 7900HT Real-Time PCR System (Applied Biosystems, Framingham, MA). Threshold cycle values, Ct, were determined to estimate differences in starting cDNA copy number that resulted from loading or other treatments. Glyceraldehyde-3-phosphate dehydrogenase (GAPDH) expression was used for normalization. The primers used were as follows: Col I (forward primer, 5′-GGAGAGAGTGCCAACTCCAG-3′; reverse primer, 5′-GTGCTTTGGAAAATGGTGCT-3′); Col III (forward primer, 5′-AGGCCAATGGCAATGTAAAG-3′; reverse primer, 5′-TGTCTTGCTCCATTCACCAG-3′); Col V (forward primer, 5′-ACCTGTTCAAAGCGAAATGG-3′; reverse primer, 5′-TTCAAAGCCAAATTCCTGGTC-3′).

Statistical analysis: Changes in tangent stiffness ($T_{1\rightarrow 2}$) and hysteresis ($H_{1\rightarrow 2}$) were assessed with Wilcoxon Rank Sum test (difference from zero) within each damage level, and Kruskal–Wallis test with post-hoc Dunn (SPSS software, Chicago, IL, USA) assessed difference between fatigue damage levels. A two-way ANOVA was used to compare mRNA expression of control, sham, Low-, Moderate-, and High-level fatigue loaded and lacerated tendons at all time points. Significant relationships identified with two-way ANOVA were further analyzed with Kruskal–Wallis test with Dunn's post-hoc test. Statistical significance was set at $p<0.05$.

3. Results

3.1. Animal model

At completion of the loading protocol, gross inspection of the knee joint and the patellar tendon showed no damage from clamping. Rats resumed normal cage activity with no evidence of lameness or inability to use the loaded limb within 2 h of recovery. At all time points, there was no gross evidence of acute inflammation at the gripping sites or in the tendon. Incision sites showed only normal granulation tissue.

3.2. Biomechanics

No tendons failed during the course of fatigue loading. Tendons were loaded for 2232±768, 10579±8487 and 16997±10734 cycles to reach Low-, Moderate-, and High-level fatigue, respectively. For all fatigue levels, stiffness and hysteresis significantly changed from baseline to endpoint states ($p\leq 0.001$). Specifically, endpoint stiffness increased by 18.3±10.6% and 18.5±9.4% and hysteresis decreased by 30.1±10.7% and 29.6±7.1% at Low and Moderate levels of fatigue, respectively. In contrast, at High-level fatigue, stiffness decreased by 17.0±6.8% and hysteresis increased by 25.3±18.5% from baseline levels. Changes in stiffness and hysteresis significantly differed between High and both lower fatigue levels (Fig. 4) ($p\leq 0.001$).

3.3. Microstructural studies

SHG images showed highly detailed collagen fibril architecture. Control tendons exhibited highly aligned, parallel collagen fibrils–fibers, with no matrix disruption (Fig. 5A). At Low fatigue, tendon microstructure exhibited isolated *kinked* fiber patterns (Fig. 5B). At Moderate fatigue, there was an increase in matrix disruptions and angulated fiber patterns (Fig. 5C), with widened interfiber spaces. At High fatigue, there was greater interfiber space widening and severe matrix disruption (Fig. 5D) with major fiber angulations, thinning, and discontinuities.

3.4. Gene expression

Generally, changes in collagen gene expression were modest at Low and Moderate damage levels in comparison with High damage levels (Fig. 6). Since no significant differences were found between the 1 and 3-day sham groups, these data were pooled. At these levels, in comparison to control/sham, Col I expression was downregulated by 1.8-fold ($p=0.001$) at 1-day and 1.5-fold ($p=0.018$) at 3-day post-fatigue at Low level damage, but did not differ at either time point ($p\geq 0.64$) for Moderate level damage. At High damage level, Col I expression increased by 4.5-fold at 1 day and then 9.9-fold at 3-days post-fatigue ($p<0.001$). Col III was upregulated by 2.8- to 4.0-fold ($p\leq 0.002$) at 1-day post-fatigue for Low and Moderate damage levels but at 3-day post-fatigue, did not differ from control/sham for Low damage levels ($p=0.9$), and decreased by 2.9-fold for Moderate damage level ($p=0.001$). At High damage level, Col III expression did not differ from control/sham at 1 day, but increased by 9.5-fold by 3-days post-fatigue ($p<0.001$). Finally, Col V was upregulated by

3.5-fold at 1-day and 3.2- to 5.8-fold at 3-day post-fatigue at Low and Moderate damage levels ($p \leq 0.020$) but was increased by 16-fold and 21-fold at 1- and 3-day post-fatigue at High damage level, respectively ($p < 0.001$).

Unlike the changes in expression of collagens in response to fatigue loading, surgically repaired lacerated tendons showed a significant change only in Col I expression, which was upregulated by 1.4-fold ($p = 0.012$) at 3-days post-fatigue. Col I at 1-day and Col III and V at both time points did not differ from control/sham levels ($p \geq 0.210$). Expression of all examined collagens were significantly lower than those at High fatigue damage level ($p < 0.001$).

4. Discussion

We developed an in vivo model in which rat patellar tendons were fatigue loaded to precisely defined levels of cumulative damage to explore mechanisms of tendon degeneration. Results showed that low level fatigue damage is represented by isolated kinked fiber patterns that transversely span across several fibers. In mid-fatigue life, tendons exhibited a greater density of deformation patterns. Surprisingly at Low- and Mid-levels, tendon damage caused increased stiffness and decreased hysteresis, likely attributable to fiber recruitment that redistributes loads from damaged to undamaged fibers during cyclic loading (Thornton et al., 2003). Despite the absence of stiffness loss, local plastic deformation is structurally reflected by an increase in peak cyclic strain, which defined the levels of damage in this study. Loading to High-level resulted in severe damage, reduction in stiffness and increase in energy dissipation in conjunction with a steep increase in tendon strain. With further loading, damage accumulation will inevitably lead to rupture.

Microstructural and biomechanical results support the effectiveness of our in vivo rat patellar tendon model in inducing matrix damage. Morphological analysis demonstrated similar tendon microstructural characteristics previously shown in ex vivo studies at comparable stages of fatigue life (Fung et al., 2008). Similarities between morphologic findings presented in this study and those of human tendon pathology and injury (Kannus and Jozsa, 1991; Kastelic and Baer, 1980; Sonnabend et al., 2001; Torp and Baer, 1975) support the role of damage accumulation in the pathogenesis of tendinopathy. In this study, the observed degradation of mechanical properties that accompanied damage accumulation is consistent with findings that overuse of the supraspinatus tendon induces mechanical degradation (Soslowsky et al., 2000).

At Low, Moderate and High fatigue, significant changes in expression of collagens were observed. Specifically, acute responses of Col I, Col III and Col V were consistent with those previously shown of tendon injury and pathology. Others reported increases in Col III and V, and decrease in Col I in biopsied specimens of posterior tibial tendon dysfunction syndrome based on immunohistological (Satomi et al., 2008) and protein expression analysis (Goncalves-Neto et al., 2002). At High fatigue level, severe matrix disruption was accompanied by increase in Col I (4.5-fold), Col III (9.5-fold) and Col V (20 fold). The observed downregulation of Col I and upregulation of Col III and Col V in the Low damage group characterizes the molecular responses in the early stages of development of tendon damage accumulation. At this time progression, molecular analyses suggests a response that prompts for scar tissue deposition without Type I collagen fibrillogenesis. While this is inconsistent with tendon healing post-laceration, the response of the tendon to early fatigue damage accumulation at Low Moderate damage levels was also not consistent with that of a repair response. This study suggests that a molecular post-fatigue repair response may not be mounted until reaching higher fatigue damage levels.

In contrast to the variable changes in the expression of collagens in fatigue damaged tendons, repaired lacerated tendons demonstrated significant increase in expression of Col I only. This difference in molecular response may be attributable to global microdamage accumulation in comparison to the localized midsubstance injury in laceration-repair models. Additional experiments are underway to determine the extent to which changes in gene expression result in tissue repair.

In this study, we implemented an advanced imaging technique (SHG imaging) which shows tendon morphology at the fiber–fibril level by detecting a nonlinear optical property inherent to fibrillar collagen. SHG imaging demonstrated that fatigue damage is characterized by fiber angulation (increasing in density with damage level) and *delamination* among adjacent fibers. Future studies will investigate the 3 D distribution and formation of these damage patterns. In this study, SHG imaging advanced our understanding of the microstructural response that underlies fatigue damage accumulation.

A limitation of our experimental approach is that the *acute* fatigue loading regime does not accurately simulate a chronic injury as there are ethical limitations to the amount of time in a single bout of loading that the animals can be anethesized for fatigue loading induction. Nonetheless, our developed model can provide valuable insights into the cumulative damage process, since the loading protocol allows us to *titrate* the amount of induced fatigue damage reliably in the tendon. This circumvents the limitation imposed by loading regimes such as treadmill running and repetitive reaching tasks where the induced loading likely varies among animals. In addition, our molecular studies were performed only at 1- and 3-days post-fatigue, and despite insight gained into differences in gene expressions response for different levels of damage, additional time points post-fatigue would provide insight into the tendon's response. Furthermore, to molecularly characterize the novel tendon fatigue model, this study focused on early phase mRNA expression response of Col I, III and V. Future studies will utilize this model to investigate an array of gene expression profiles and proteomic changes of both anabolic and catabolic molecules at different time points post-fatigue induction.

In conclusion, we developed a novel, in vivo rat patellar tendon model of damage accumulation to evaluate the microstructural, mechanical and biological response to fatigue damage. Progressive levels of sub-rupture matrix damage were induced in the tendon based on increases in tendon strain. SHG imaging revealed characteristic morphological damage in tendon microstructure in the progression of early- to late-stage fatigue. Analysis of mRNA expression showed modest changes in Col I, III and V at early- and mid-stage fatigue life and greater changes for late fatigue life, while tendon stiffness decreased only in late fatigue life. Fatigue-induced changes in both morphology and molecular profile (at early and mid stages of fatigue in our model) are consistent with pathologic features of human tendon degeneration. Findings provide evidence of fatigue loading as a pathomechanical factor of wear and tear tendinopathy and indicate that tendons elicit a molecular response to sub-rupture fatigue damage accumulation.

Acknowledgments

This study was supported by Aircast Foundation and NIH (AR41210, AR44927, AR49967, and AR52743).

References

Backman C, Boquist L, Friden J, Lorenzon R, Toolanen G. Chronic achilles paratenonitis with tendinosis: an experimental model in the rabbit. J Orthop Res. 1990; 8 (4):541–547. [PubMed: 2355294]

Fung DT, Wang VM, Laudier DM, Shine JH, Basta-Pljakic J, Jepsen KJ, Schaffler MB, Flatow EL. Subrupture tendon fatigue damage. J Orthop Res. 2008

Goncalves-Neto J, Witzel SS, Teodoro WR, Carvalho-Junior AE, Fernandes TD, Yoshinari HH. Changes in collagen matrix composition in human posterior tibial tendon dysfunction. Jt Bone Spine. 2002; 69 (2):189–194.

Hiranuma K, Suzuki K, Hirata K, Nakamura H, Higashi K, Hirano H. Extracellular matrices in peritendinous connective tissue after surgical injury to the chicken flexor tendon. Arch Orthop Trauma Surg. 1996; 115 (2):63–77. [PubMed: 9063853]

Jepsen KJ, Davy DT. Comparison of damage accumulation measures in human cortical bone. J Biomech. 1997; 30 (9):891–894. [PubMed: 9302611]

Kannus P, Jozsa L. Histopathological changes preceding spontaneous rupture of a tendon. A controlled study of 891 patients. J Bone Jt Surg Am. 1991; 73 (10):1507–1525.

Kastelic J, Baer E. Deformation in tendon collagen. Symp Soc Exp Biol. 1980; 34:397–435. [PubMed: 7256561]

Ker RF, Wang XT, Pike AV. Fatigue quality of mammalian tendons. J Exp Biol. 2000; 203 (Part 8): 1317–1327. [PubMed: 10729280]

Laudier D, Schaffler MB, Flatow EL, Wang VM. Novel procedure for high-fidelity tendon histology. J Orthop Res. 2007; 25 (3):390–395. [PubMed: 17149746]

Leadbetter WB. Cell–matrix response in tendon injury. Clin Sports Med. 1992; 11 (3):533–578. [PubMed: 1638640]

Lin TW, Cardenas L, Soslowsky LJ. Biomechanics of tendon injury and repair. J Biomech. 2004; 37 (6):865–877. [PubMed: 15111074]

Maffulli N, Testa V, Capasso G, Ewen SW, Sullo A, Benazzo F, King JB. Similar histopathological picture in males with Achilles and patellar tendinopathy. Med Sci Sports Exer. 2004; 36 (9):1470–1475.

Maganaris CN, Narici MV, Almekinders LC, Maffulli N. Biomechanics and pathophysiology of overuse tendon injuries: ideas on insertional tendinopathy. Sports Med. 2004; 34 (14):1005–1117. [PubMed: 15571430]

Matheson GO. Long-term prognosis for jumper's knee. Clin J Sport Med. 2003; 13 (3):196. [PubMed: 12795300]

Mehta S, Gimbel JA, Soslowsky LJ. Etiologic and pathogenetic factors for rotator cuff tendinopathy. Clin Sports Med. 2003; 22 (4):791–812. [PubMed: 14560548]

Nakama LH, King KB, Abrahamsson S, Rempel DM. Evidence of tendon microtears due to cyclical loading in an in vivo tendinopathy model. J Orthop Res. 2005 in press.

Oshiro W, Lou J, Xing X, Tu Y, Manske PR. Flexor tendon healing in the rat: a histologic and gene expression study. J Hand Surg [Am]. 2003; 28 (5):814–823.

Pike AV, Ker RF, Alexander RM. The development of fatigue quality in high- and low-stressed tendons of sheep (Ovis aries). J Exp Biol. 2000; 203 (Part 14):2187–2193. [PubMed: 10862730]

Ralphs JR, Benjamin M, Waggett AD, Russell DC, Messner K, Gao J. Regional differences in cell shape and gap junction expression in rat Achilles tendon: relation to fibrocartilage differentiation. J Anat. 1998; 193 (Part 2):215–222. [PubMed: 9827637]

Riley G. The pathogenesis of tendinopathy. A molecular perspective. Rheumatology (Oxford). 2004; 43 (2):131–142. [PubMed: 12867575]

Sakai H, Koibuchi N, Ohtake H, Tamai K, Fukui N, Oda H, Saotome K. Type I and type III procollagen gene expressions in the early phase of ligament healing in rabbits: an in situ hybridization study. J Orthop Res. 2001; 19 (1):132–135. [PubMed: 11332609]

Satomi E, Teodoro WR, Parra ER, Fernandes TD, Velosa AP, Capelozzi VL, Yoshinari NH. Changes in histoanatomical distribution of types I, III and V collagen promote adaptative remodeling in posterior tibial tendon rupture. Clinics. 2008; 63 (1):9–14. [PubMed: 18297201]

Schechtman H, Bader DL. In vitro fatigue of human tendons. J Biomech. 1997; 30 (8):829–835. [PubMed: 9239568]

Schechtman H, Bader DL. Fatigue damage of human tendons. J Biomech. 2002; 35 (3):347–353. [PubMed: 11858810]

Sonnabend DH, Yu Y, Howlett CR, Harper GD, Walsh WR. Laminated tears of the human rotator cuff: a histologic and immunochemical study. J Shoulder Elbow Surg. 2001; 10 (2):109–115. [PubMed: 11307072]

Soslowsky LJ, Thomopoulos S, Tun S, Flanagan CL, Keefer CC, Mastaw J, Carpenter JE. Neer Award 1999. Overuse activity injures the supraspinatus tendon in an animal model: a histologic and biomechanical study. J Shoulder Elbow Surg. 2000; 9 (2):79–84. [PubMed: 10810684]

Tallon C, Maffulli N, Ewen SW. Ruptured Achilles tendons are significantly more degenerated than tendinopathic tendons. Med Sci Sports Exer. 2001; 33 (12):1983–1990.

Thornton GM, Shrive NG, Frank CB. Healing ligaments have decreased cyclic modulus compared to normal ligaments and immobilization further compromises healing ligament response to cyclic loading. J Orthop Res. 2003; 21 (4):716–722. [PubMed: 12798073]

Torp, S.; Baer, E.; Friedman, B. Effects of age and of mechanical deformation on the ultrastructure of tendon. In: Atkins, EDT.; Keller, A., editors. Structure of Fibrous Biopolymers. Butterworths; London: 1975. p. 223-250.

Wang XT, Ker RF. Creep rupture of wallaby tail tendons. J Exp Biol. 1995; 198 (3):831–845. [PubMed: 9244804]

Wang XT, Ker RF, Alexander RM. Fatigue rupture of wallaby tail tendons. J Exp Biol. 1995; 198 (3): 847–852. [PubMed: 9244805]

Williams IF, McCullagh KG, Silver IA. The distribution of types I and III collagen and fibronectin in the healing equine tendon. Connect Tissue Res. 1984; 12 (3–4):211–227. [PubMed: 6478822]

Wren TA, Lindsey DP, Beaupre GS, Carter DR. Effects of creep and cyclic loading on the mechanical properties and failure of human Achilles tendons. Ann Biomed Eng. 2003; 31 (6):710–717. [PubMed: 12797621]

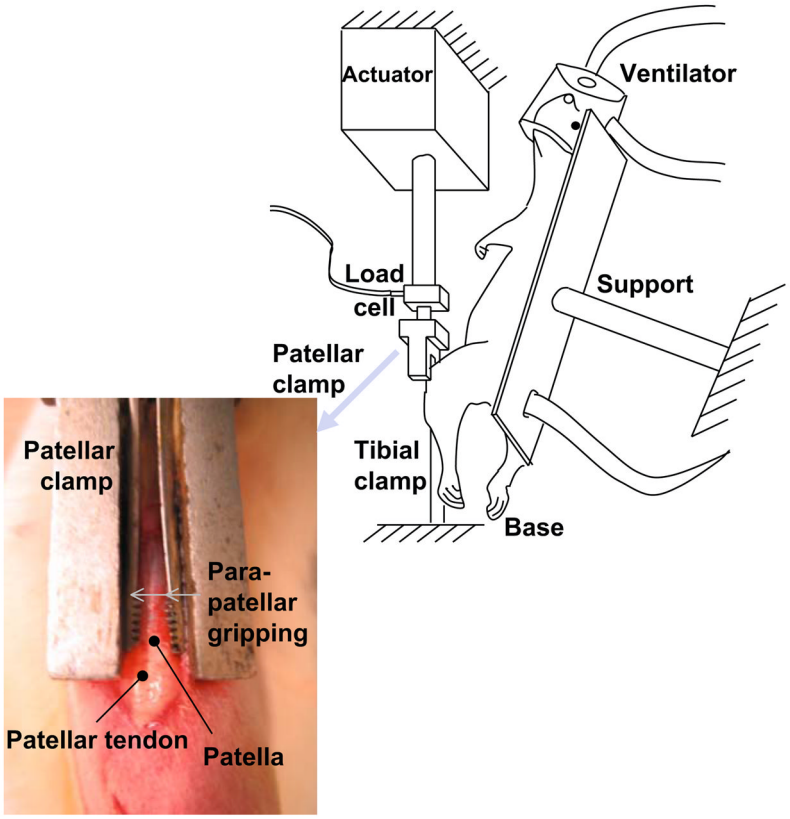

Fig. 1.
Experimental setup. The anesthetized rat was fixed onto support. Custom-made clamps connected the patella to a load cell and the tibia to a base, allowing tendon loading without contact with the tendon.

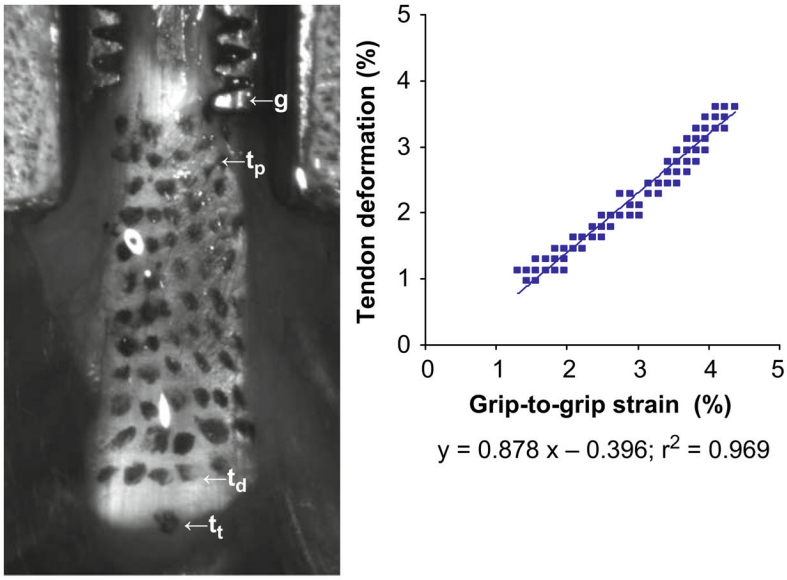

Fig. 2.

Calibration of actuator movement with tendon deformation. A grid of ink dots were applied to the tendon surface. Deformation was determined from change in position between dots on the proximal (t_p) and distal end (t_d) of the tendon from images recorded during loading. Actuator (grip-to-grip) strain was determined from changes in positions between t_d and g, a location on the patellar grip rigidly attached to the actuator. Linear regression between tendon deformation and actuator strain is characterized by a slope of 0.878 and r^2 of 0.969.

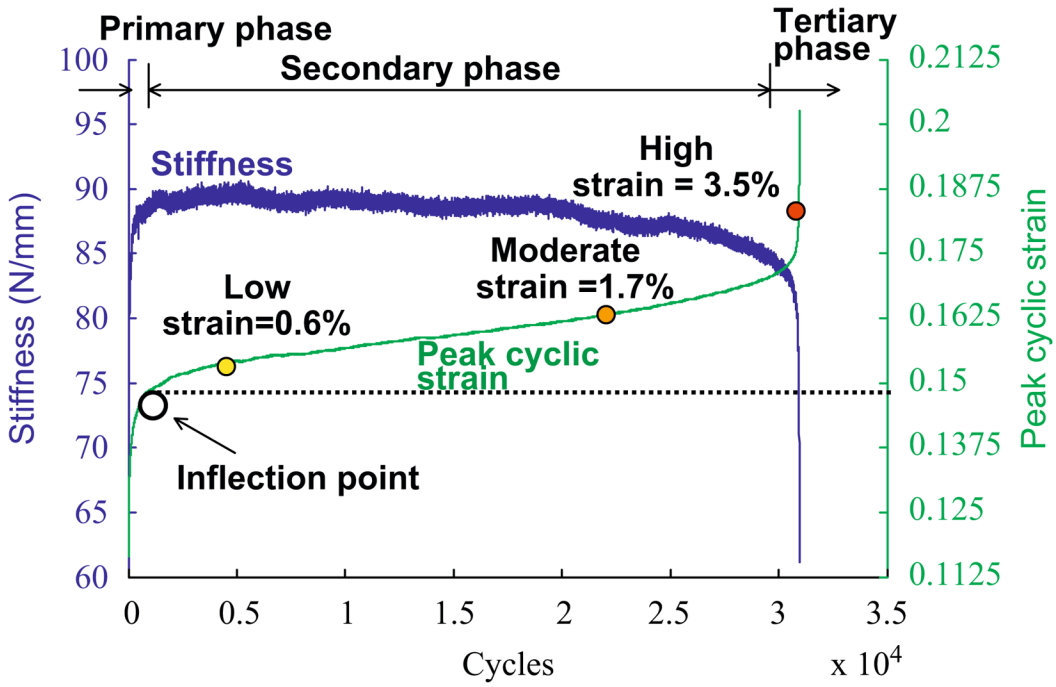

Fig. 3.

Representative loading history. Stiffness and peak cyclic strain follow different triphasic patterns during the tendon fatigue life. Stiffness increases rapidly in the Primary phase, reaches a relatively constant level in the Secondary phase, leading to an accelerating rate of decline in the Tertiary phase. In contrast, peak cyclic strain increases rapidly in the Primary phase, reaching a slow and steady rate of increase in the Secondary phase, followed by an accelerated rate of increase in the Tertiary phase. Fatigue damage levels are set at 0.6% (Low), 1.7% (Moderate) and 3.5% (High) strain increase from initial measurement determined at cycle 500, which occurs beyond the inflection point, the transition between the Primary and Secondary phase.

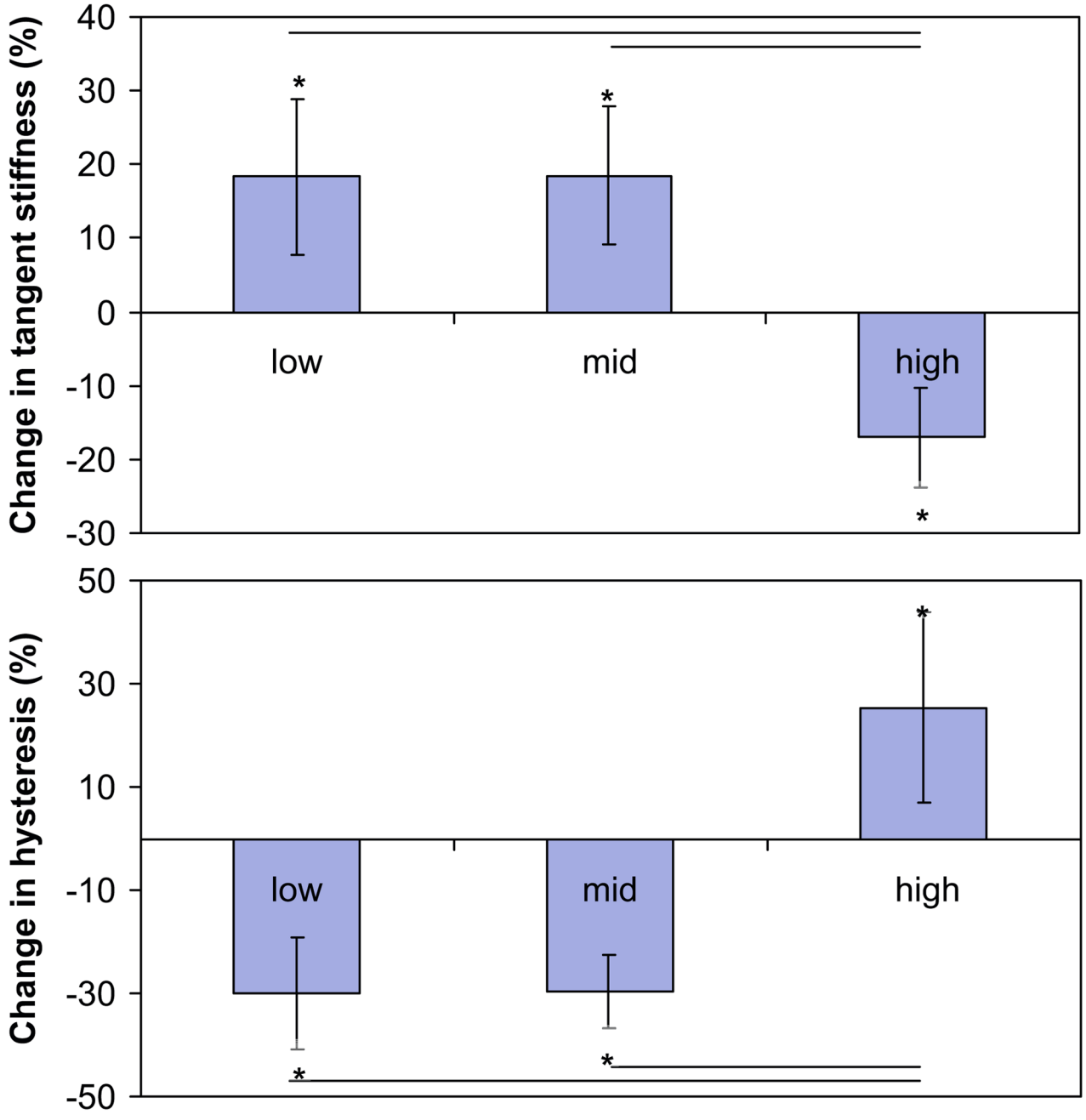

Fig. 4.

Within each fatigue damaged level, mechanical properties changed significantly from baseline cycle to endpoint cycle (* denotes $p<0.05$). At both Low and Moderate fatigue, stiffness increased and hysteresis decreased. Conversely, at High fatigue, stiffness loss and hysteresis increase were observed. Changes in both stiffness and hysteresis were significant between High and the lower levels of fatigue (— denotes $p<0.05$).

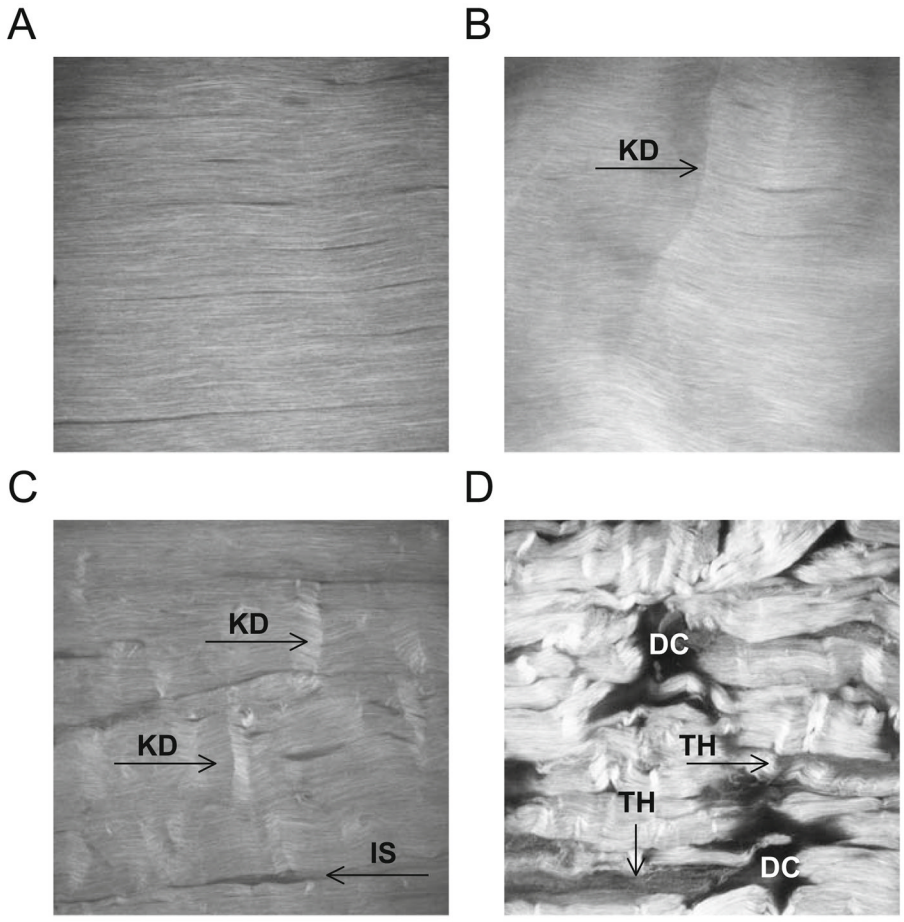

Fig. 5.

Multiphoton microscopy of tendons. (A) Control tendons exhibited highly aligned, parallel collagen fibrils–fibers without matrix disruption. At Low fatigue (B), tendon microstructure featured isolated *kinked* fiber deformations (KD) that span transversely across several fibers. At Moderate fatigue (C), density of damage patterns in the matrix and widening of the interfiber space (IS) increased. At High fatigue (D), there was severe matrix disruption, poor fiber alignment, and greater widening of interface space. Regions of low signal intensity suggest fiber thinning (TH) and more severely, matrix discontinuities (DC). FOV=400 mm.

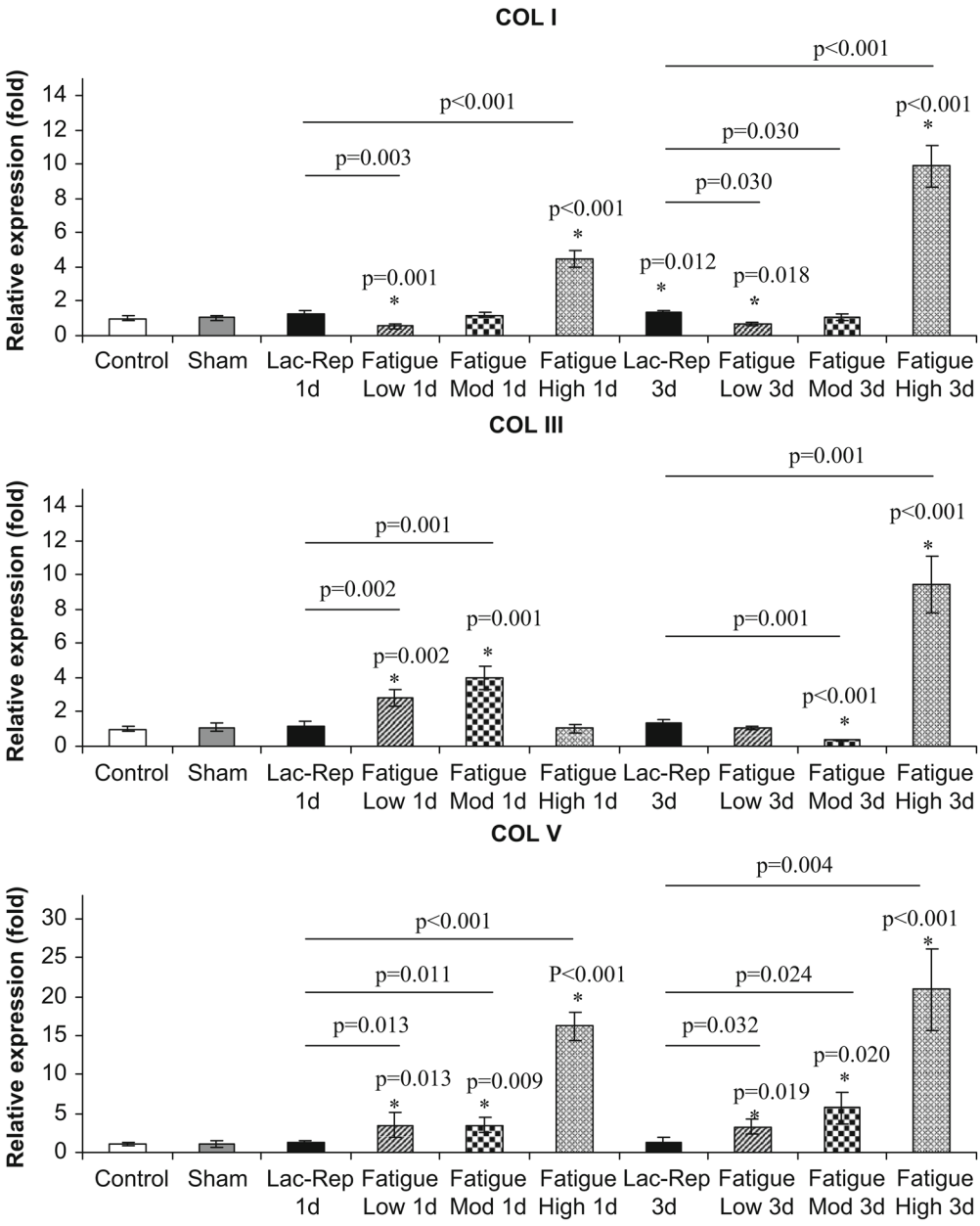

Fig. 6.

Molecular responses. Real-time PCR analysis of mRNA expression of Col I, III and V demonstrated differences in molecular responses between laceration-repair and fatigue damage at various levels (* denotes expression levels of laceration or fatigue groups that exhibit significant relationships with control/sham groups; — denotes significant relationships between fatigue damage and laceration-repaired groups).